



## COVID19-inhibitory activity of withanolides involves targeting of the host cell surface receptor ACE2: insights from computational and biochemical assays

Rajkumar Singh Kalra<sup>a</sup>, Vipul Kumar<sup>b</sup>, Jaspreet Kaur Dhanjal<sup>a</sup>, Sukant Garg<sup>a</sup>, Xiaoshuai Li<sup>a</sup>, Sunil C. Kaul<sup>a</sup>, Durai Sundar<sup>b</sup> and Renu Wadhwa<sup>a</sup>

<sup>a</sup>Cellular and Molecular Biotechnology Research Institute, AIST-INDIA DAILAB, DBT-AIST International Center for Translational & Environmental Research (DAICENTER), National Institute of Advanced Industrial Science & Technology (AIST), Japan; <sup>b</sup>DAILAB, Department of Biochemical Engineering & Biotechnology, Indian Institute of Technology (IIT) Delhi, Hauz Khas, New Delhi, India

Communicated by Ramaswamy H. Sarma

### ABSTRACT

SARS-CoV-2 outbreak in China in December 2019 and its spread as worldwide pandemic has been a major global health crisis. Extremely high infection and mortality rate has severely affected all sectors of life and derailed the global economy. While drug and vaccine development have been prioritized and have made significant progression, use of phytochemicals and herbal constituents is deemed as a low-cost, safer and readily available alternative. We investigated therapeutic efficacy of eight withanolides (derived from Ashwagandha) against the angiotensin-converting enzyme 2 (ACE2) proteins, a target cell surface receptor for SARS-CoV-2 and report results on the (i) computational analyses including binding affinity and stable interactions with ACE2, occupancy of ACE2 residues in making polar and nonpolar interactions with different withanolides/ligands and (2) *in vitro* mRNA and protein analyses using human cancer (A549, MCF7 and HSC3) cells. We found that among all withanolides, Withaferin-A, Withanone, Withanoside-IV and Withanoside-V significantly inhibited the ACE2 expression. Analysis of withanolides-rich aqueous extracts derived from Ashwagandha leaves and stem showed a higher ACE2 inhibitory potency of stem-derived extracts. Taken together, we demonstrated the inhibitory potency of Ashwagandha withanolides and its aqueous extracts against ACE2.

### ARTICLE HISTORY

Received 25 January 2021  
Accepted 9 March 2021

### KEYWORDS





Coronavirus; SARS-CoV-2; COVID-19; *Withania somnifera*; Ashwagandha; withanolides; angiotensin-converting enzyme 2; inhibition


## 1. Introduction

The coronavirus disease 19 (COVID-19), emerged in the Hubei province of China has become a worldwide pandemic affecting 219 countries with an estimate of more than 103 million infected cases and over 2.4 million deaths (WHO Coronavirus Disease [COVID-19] Dashboard, as on 16 February 2021; <https://covid19.who.int/>). The novel severe acute respiratory syndrome coronavirus-2 (SARS-CoV-2), the causative agent of COVID-19, belongs to the class of beta-coronaviruses that have a history of infecting humans through birds and mammals and has a trend similar to the past pandemics caused by severe acute respiratory syndrome coronavirus (SARS-CoV) and middle east respiratory syndrome coronavirus (MERS-CoV) (Lu et al., 2020). Although enormous efforts are being taken worldwide, only a few treatment options available so far include the use of remdesivir, lopinavir + ritonavir, lopinavir + ritonavir + interferon beta-1 $\alpha$  or hydroxychloroquine (WHO, 2020) (Kalra et al., 2020).

SARS-CoV-2 is a positive sense RNA virus made up of four structural proteins-envelope (E), membrane (M), nucleocapsid (N) and spike (S) protein (Rota et al., 2003). Spike

glycoprotein is one of the key players directly involved in the infection cycle of this virus (Hulswit et al., 2016). The S proteins exist on the surface of the viral particle as homotrimers giving it a crown like appearance (Tortorici & Veesler, 2019). Each of the S protein consists of two subunits, S1 and S2. The S1 subunit directly interacts with the host cell surface receptors via its receptor-binding domain while the S2 subunit facilitates the fusion of the viral particle and the host cell membrane (Tai et al., 2020). SARS-CoV-2 uses angiotensin-converting enzyme-2 (ACE2) receptor as the main anchorage point (Letko et al., 2020; Zhou et al., 2020). However, the entry of SARS-CoV-2 into the host cells is possible only after the priming of this S protein at the S1/S2 and the S2' site by another host cell protease receptor called transmembrane protease serine 2 (TMPRSS2) (Hoffmann et al., 2020). Another recent report has shown the involvement of heparan sulfates as well in the process of the ACE2 mediated SARS-CoV-2 entry into the host cells (Clausen et al., 2020; Kalra & Kandimalla, 2021; Zhang et al., 2020). ACE2, thus, forms the primary check point to stop the transmission and infection of SARS-CoV-2 and is a promising molecular target for investigating new SARS-CoV-2 infection prevention strategies.

**CONTACT** Durai Sundar  [sundar@dbeb.iitd.ac.in](mailto:sundar@dbeb.iitd.ac.in)  DAILAB, Department of Biochemical Engineering & Biotechnology, Indian Institute of Technology (IIT) Delhi, Hauz Khas, New Delhi 110 016, India; Renu Wadhwa  [renu-wadhwa@aist.go.jp](mailto:renu-wadhwa@aist.go.jp)  Cellular and Molecular Biotechnology Research Institute, AIST-INDIA DAILAB, National Institute of Advanced Industrial Science & Technology (AIST), Tsukuba 305 8565, Japan

 Supplemental data for this article can be accessed online at <https://doi.org/10.1080/07391102.2021.1902858>

ACE2 is a type I membrane protein expressed mainly in lung, kidney, intestine and heart (Donoghue et al., 2000; Li et al., 2020). A series of crystal structures of the receptor binding domain of SARS-CoV with ACE2 have been reported previously. It was found that the surface of ACE2 contains two virus-binding hotspots, which are crucial for interaction with the S protein of SARS-CoV. Mutations surrounding these hotspots have been demonstrated to dictate the infectivity, pathogenesis and cross-species and human-to-human transmissions of these viral particles (Li, 2008; Li et al., 2005; Wu et al., 2012). On the basis of this information, differences between the binding of SARS-CoV and SARS-CoV-2 to ACE2 have also been studied (Ali & Vijayan, 2020). The Receptor Binding Domain (RBD) region of SARS-CoV and SARS-CoV-2 shows a sequence similarity of 73–76% (Wan et al., 2020). Fourteen residues of the SARS-CoV (Tyr436, Tyr440, Tyr442, Leu443, Leu472, Asn473, Tyr475, Asn479, Gly482, Tyr484, Thr486, Thr487, Gly488 and Tyr4918) have been reported to be involved in binding with ACE2 (Li et al., 2005; Walls et al., 2020). Only eight (Tyr449, Tyr453, Asn487, Tyr489, Gly496, Thr500, Gly502 and Tyr505) of these 14 residues were found to be conserved in SARS-CoV-2 RBD domain. SARS-CoV-2 also possesses a higher binding affinity for ACE2 in comparison to SARS-CoV (Lan et al., 2020; Wang et al., 2020), and this has been attributed to substitutions observed at Leu455, Phe456, Phe486, Gln493, Gln498 and Asn501. Amongst these, Gln493 and Asn501 (Asn479 and Thr487 in SARS-CoV) are located near viral binding hotspot residues Lys31 and Lys353 on human ACE2 that favors the binding of SARS-CoV-2 to ACE2. This interaction is further strengthened by the binding of Leu455, Phe486 and Gln498 (Wan et al., 2020). Furthermore, the crystal structure of human ACE2 bound to S protein of SARS-CoV-2 showed a network of hydrophilic interactions including 13 hydrogen bonds and 2 salt bridges (Lan et al., 2020). These data have uncovered the interaction interface between SARS-CoV-2 and ACE2, thereby paving the way for structure-based rational drug design and discovery. Drug repositioning or drug repurposing has opened up more opportunities in this current pandemic situation. The use of known drug candidates does not only reduce the time required for chemical–structural optimization, but can also account for the toxicological testing.

Ashwagandha (*Withania somnifera*) is a herb extensively used in the Indian traditional medicine system called Ayurveda. It has been well documented for its therapeutic activities and immunity boosting potential. We have previously reported the anticancer activity of two of its major bioactive components: Withaferin-A and Withanone. The anticancer activity has been shown to be mediated through multiple mechanisms, mainly including activation of tumor suppressor proteins, p53 and pRB, inactivation of NF- $\kappa$ B, Aurora A, DNA damage repair and oxidative stress (Bhargava et al., 2019; Gao et al., 2014; Grover, Priyandoko, et al., 2012; Grover, Singh, et al., 2012; Sundar et al., 2019; Widodo et al., 2007, 2010; Yu et al., 2017). These withanolides have also been studied for their anti-viral effects. Withaferin-A has been previously reported to be effective against herpes simplex virus, HIV and H1N1 influenza virus (Cai et al., 2015; Grover et al., 2011; Shi et al., 2017). We have earlier demonstrated the effect of Withaferin-A and Withanone on

TMPRSS2 (required for SARS-CoV-2 entry into the host cells) (Kumar, Dhanjal, Bhargava, et al., 2020). Furthermore, the main protease ( $M^{pro}$ ) of SARS-CoV-2 that is essential for its replication in host cells was also predicted to be a potential target for Withanone (Kumar, Dhanjal, Kaul, et al., 2020). In view of this information, in this study, we attempted to investigate COVID-19 inhibitory potential of different withanolides (at sub-cytotoxic doses) found in Ashwagandha with respect to their interactions mainly with ACE2 host cell surface receptor. Using computational and experimental approaches, we examined the effect of eight withanolides (Withaferin-A, Withanone, Withanolide-A, Withanolide-B, Withanoside-IV, Withanoside-V, methoxyWithaferin-A and 12-deoxywithanostaminolide). The binding affinity and molecular interaction of withanolides with ACE2 have also been compared to an already reported clinical trial candidate drug viz. Umifenovir against ACE2. We report that among all the tested withanolides, Withaferin-A, Withanone, Withanoside-IV, Withanoside-V showed ACE2 inhibitory activity in *in vitro* assays. Furthermore, water-based extracts from Ashwagandha stem showed remarkable activity, and hence, are suggested to offer a useful resource for COVID-19 treatment and future drug development.

## 2. Materials and methods

### 2.1. Preparation of the ACE2 and ligands structures

The structure of SARS-CoV-2 Spike protein (Receptor Binding Domain) in complex with ACE2 receptor, resolved using X-ray diffraction (resolution of 2.5 Å), was downloaded from RCSB Protein Data Bank (PDB ID: 6LZG) (Wang et al., 2020). The crystal structure was visualized to investigate the critical residues of the ACE2 that were making hydrogen bonds with the Spike protein (Figure 1). It was found that in the native crystal structure, Ser19, Gln24, Lys34, Glu35, Asp38 and Gln42 of ACE2 were making contact with the Spike protein. Further, the crystal structure was prepared for docking using protein preparation wizard of the maestro (Madhavi Sastry et al., 2013; Schrödinger, 2020). The preparation steps involved addition of missing disulfide bonds, removal of water molecules, addition of missing hydrogen atoms, filling of missing amino acids side chains and optimization of hydrogen bonds. The OPLS3e forcefield was then used for restrained minimization until the average root mean square deviation (RMSD) of the non-hydrogen atoms converged to 0.30 Å (Harder et al., 2016). After protein preparation, the ligands Umifenovir (CID 131411), Withanoside-V (CID 10700345), methoxyWithaferin-A (CID 10767792), Withanolide-A (CID 11294368), Withanolide-B (CID 14236711), 12-deoxywithastramonolide (CID 44576309), Withaferin-A (CID 265237), Withanone (CID 21679027) and Withanoside-IV (CID 71312551) were retrieved from PubChem database and were prepared using the LigPrep tool of the Schrodinger suite (Supporting Information Figure S1) (Madhavi Sastry et al., 2013; Schrödinger, 2020).

### 2.2. Molecular docking of the ligands with ACE2

The grid of 20 Å was generated by covering ACE2 residues that were making hydrogen bonds with Spike protein in the

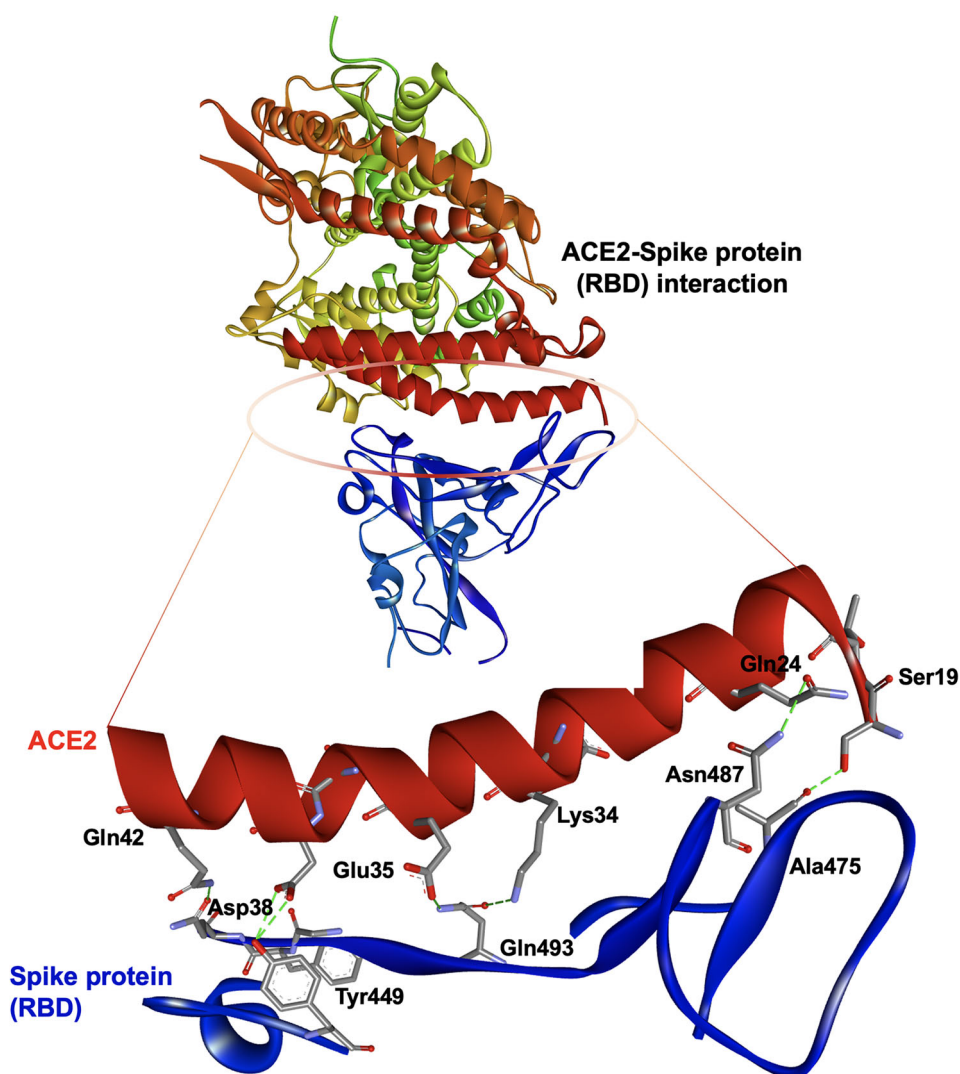


**Figure 1.** The binding interaction between ACE2 and Spike protein's Receptor Binding Domain (RBD) showing the crucial residues making hydrogen bond in the native crystalized structure (PDB ID 6LZG).

native crystal structure (mainly involving Ser19, Gln24, Lys34, Glu35, Asp38 and Gln42). The Glide module of Schrodinger was used for the extra precision (XP) flexible docking of the ligands within the generated grid site on ACE2 (Friesner et al., 2006). AutoDock Vina was also used to re-assess the docked confirmations (Pagadala et al., 2017).

### 2.3. Molecular dynamics simulation in water

To investigate the binding stability and interactions between the protein and ligands, the docked complexes were subjected to classical molecular dynamics (MD) simulations. The MD simulations were performed using the Desmond tool integrated with the maestro of Schrodinger suite (Schrodinger, 2020). Each protein–ligand system was solvated in the TIP3P water model. Further, the solvated systems were neutralized by adding appropriate counter ions and then the energy of the systems was minimized for 5000 steps using the steepest descent method. The minimized systems were equilibrated using the 'Relax Model scheme' in the Desmond, which performed the NPT/NVT equilibration. The equilibrated

systems were then subjected to 100 ns of the MD production run in NPT ensemble at 300K temperature using Noose–Hoover thermostat, 1atm pressure using the Martyna–Tobias–Kelin barostat, 2 fs integration time step and recording interval of 20 ps.

The simulated systems were analysed for the Root Mean Square Deviation (RMSD), Root Mean Square Fluctuation (RMSF), Hydrogen bond counts and interaction occupancies using simulation event analysis and simulation interaction diagram tool of Desmond module of Schrodinger. Finally, the MM/GBSA free energy was calculated for each protein–ligand system by extracting 100 structures from the simulation trajectory for the duration of 40 ns to 100 ns at an interval of 30 frames. Following equations were used for the calculation of MM/GBSA-

$$\text{MM/GBSA } \Delta G_{\text{bind}} = \Delta G_{\text{complex}} - (\Delta G_{\text{receptor}} + \Delta G_{\text{ligand}})$$

$$\Delta G = \Delta E_{\text{gas}} + \Delta G_{\text{sol}} - T\Delta S_{\text{gas}}$$

Here,  $\Delta G$  is free energy,  $\Delta E_{\text{gas}}$  is gas-phase interaction energy,  $\Delta G_{\text{sol}}$  is solvation free energy,  $T$  is temperature and  $\Delta S_{\text{gas}}$  is entropy.

**Table 1.** Details of Ashwagandha withanolides and Ashwagandha extracts used in the study.

Chemical library compounds	Code	Source/reference
DMSO	Con	0.01%
Withaferin-A	1	0.01 $\mu$ M
MethoxyWithaferin-A	2	3 $\mu$ M
Withanone	3	5 $\mu$ M
Withanolide-A	5	5 $\mu$ M
Withanolide-B	6	5 $\mu$ M
Withanoside-IV	7	5 $\mu$ M
Withanoside-V	8	5 $\mu$ M
Withanostaminolide-12-deoxy	9	3 $\mu$ M
Ash M2H1 - BCD 23 (leaf)	D76	-
Ash M2H1 - BDM 24 (leaf)	D77	-
Ash M3 - BCD 27 (stem)	D78	-
Ash M3 - BDM 28 (stem)	D79	-

The prime module of Schrodinger software was used to compute all the energy components using the coordinates of the complexes, receptor and ligands using the OPL3e forcefield and VSGB solvation model.

## 2.4. Cell culture and treatments

Human cancer cells, A549 (non-small cell lung cancer), MCF7 (human breast carcinoma) and HSC3 (oral squamous cell carcinoma) were procured from the Japanese Collection of Research Bioresources Cell Bank (JCRB), Japan. Cells were cultured in Dulbecco's modified Eagle's medium (Invitrogen)-supplemented with 5% fetal bovine serum and 1% penicillin/streptomycin in a humidified incubator (37 °C and 5% CO<sub>2</sub>). Details of chemical library compounds used for drug screening are provided in Table 1. The subtoxic concentrations of withanolides was determined for *in vitro* viability studies and as reported earlier (Antony et al., 2018; Chaudhary et al., 2017, 2019; Gao et al., 2014; Mishra et al., 2000; Sundar et al., 2019; Widodo et al., 2010).

## 2.5. Cell viability assay

Cytotoxicity of the various compounds was tested in A549, MCF7 and HSC3 cells by MTT (3-(4,5-dimethylthiazol-2-yl)-2,5-diphenyltetrazolium bromide) assay. Five thousand cells per well were plated in a 96-well plate, allowed to settle overnight and treated with each compound. The control (DMSO) or treated cells were incubated for 48 h followed by addition of 10  $\mu$ L of phosphate buffered saline (PBS) containing 5 mg/mL MTT (M6494, Life Technologies, Carlsbad, CA, USA), and further incubated for 4 h. Culture medium containing MTT was aspirated and replaced with DMSO. The plates were placed on a shaker for 5 min followed by measurement of optical density at 570 nm using Tecan infinite M200® Pro microplate reader (Tecan Group Ltd., Mannedorf, Switzerland). Cell viability was calculated as a percentage against the control to identify their Inhibitory Concentration (IC) value using Microsoft™ Office 2016. Statistical significance was calculated by an unpaired *t*-test of Microsoft Excel software (2016).

## 2.6. Reverse transcription-polymerase chain reaction

Cells (2  $\times$  10<sup>5</sup>/well) were plated in a 6-well plate, allowed to settle overnight, followed by treatment with each of

chemical library compounds. The control or treated cells were incubated at 37 °C and 5% CO<sub>2</sub>. After 48 h, the cells were harvested from the Petri dishes and lysed with Trizol (Ambion, Foster City, CA, USA, 15596018) at room temperature for 5 min, incubated in chloroform (Wako, Tokyo, Japan, 038-02606) at room temperature for 5 min, centrifuged at 12,000 rpm for 15 min. Supernatant was separated, washed in isopropanol (Wako, 166-04836) at room temperature for 10 min and centrifuged at 12,000 rpm for 15 min. The pellet was washed in 70% ice-cold ethanol and centrifuged at 8000 rpm for 5 min twice, followed by air-drying and resuspension in nuclease-free water to extract pure RNA. The concentration and quality of RNA were evaluated by a spectrophotometer (ND-1000, Nanodrops, Wilmington, NC, USA). cDNA was prepared using a reverse transcription kit (Qiagen, Hilden, Germany, 205313) following the manufacturer's instructions. The master mix for amplification was prepared by mixing 1  $\mu$ L cDNA with 0.1  $\mu$ L Ex Taq (Takara, Kusatsu, Shiga, Japan, RR001), 2  $\mu$ L 10X TAQ buffer, 2  $\mu$ L dNTP, 1  $\mu$ L each of forward and reverse primers (indicated earlier) in 12.9  $\mu$ L nuclease free water and amplified using 'denaturation = 95 °C, 10 min  $\rightarrow$  amplification = 95 °C, 45 s – 60 °C, 1 min – 72 °C, 45 s (35–37 cycles)  $\rightarrow$  annealing = 72 °C, 10 min  $\rightarrow$  4 °C' protocol. Primers used are listed in Table 2. The amplified products were resolved on a 1% agarose gel containing 0.06  $\mu$ g/mL EtBr (Ethidium Bromide; Invitrogen, 15585-011), and acquired using a Lumino Image Analyzer (LAS3000-mini; Fuji Film, Tokyo, Japan) equipped with a CCD (Charge-coupled device) camera. Band intensity was quantified using ImageJ software (NIH) and plotted as a percentage using Microsoft Office 2016. Statistical significance was calculated by an unpaired *t*-test of Microsoft Excel software (2016).

## 2.7. Immunoblotting

Cells (2.5  $\times$  10<sup>5</sup> cells/well) were plated in a 6-well plate, allowed to settle overnight, followed by treatment with each compound. The control or treated cells were incubated at 37 °C and 5% CO<sub>2</sub>. After 48 h, control and treated cells were harvested and washed with PBS (X2), followed by lysis in RIPA buffer (89900, Thermo Fisher Scientific) containing complete protease inhibitor cocktail (4693159001, Roche Applied Science, Penzberg, Bavaria, Germany) on ice for 45 min. Lysates were separated on an SDS-polyacrylamide gel using Mini-Protean Tetra cell equipment (Bio-Rad, Hercules, CA, USA), and subjected to immunoblotting using protein-specific antibodies as in Table 3, and horseradish peroxidase-conjugated secondary HRP antibody (31430 or 31460, Thermo Fisher Scientific). Blots were developed using chemiluminescence solution (GE Healthcare, Buckinghamshire, UK) and visualized using a Lumino Image Analyzer (LAS 3000-mini; Fuji Film, Tokyo, Japan). Band intensity was quantified using ImageJ software (NIH) and plotted as a percentage using Microsoft™ Office 2016. Statistical significance was calculated by an unpaired *t*-test of Microsoft Excel software (2016).

**Table 2.** Details of primers used for RT-PCR assays.

Gene	Primer sequence	Molecular weight	Cycles	Temperature (Tm)
ACE2	F'- CATTGGAGCAAGTGTGGATCTT	108 bp	38	62 °C
	R'- GAGCTAATGCATGCCATTCTCA			
GAPDH	F'- TGGAAATCCCATCACCATCT	417 bp	34	60 °C
	R'- TTCACACCCATGACGAACAT			

**Table 3.** Details of antibodies used in the study to analyze the protein expression levels.

Protein targets	Molecular weight	Source
ACE2	90-KDa	abcam (ab15348)
$\beta$ -actin	42-KDa	abcam (ab49900)

## 2.8. Statistical analyses

The data represents mean  $\pm$  SD from three independent experiments. Statistical significance was calculated by unpaired *t*-test (GraphPad Prism, GraphPad Software, San Diego, CA; *p* values \*\*\*<.001 represent highly significant change).

## 3. Results

### 3.1. Computational analysis predicted withanoside IV and withanoside V as potential inhibitors of ACE2: SARS-CoV-2 spike protein interactions

All the ligands were docked at the ACE2 binding site to investigate their best binding pose and binding energy. As many studies have reported an anti-influenza drug, Umifenovir, to be effective against ACE2-Spike protein interactions and is currently being tested in clinical trial against SARS-CoV-2 (Choudhary & Silakari, 2020; Padhi et al., 2021), so we chose this drug as a positive control for the computational study. When we docked Umifenovir at ACE2 binding site, the docking score in the best binding pose was  $-4.31$  kcal/mol and it was participating in the interaction by making hydrogen bond contacts with Lys31 and Glu35 (Figure 2(A)). In comparison to Umifenovir, Withanoside-V had the highest docking score ( $-6.29$  Kcal/mol) in the best binding pose. It was making hydrogen bonds with Lys31 and other two crucial (Glu35 and Asp38) residues that essentially play an important role in establishing contact with the RBD of SARS-CoV-2 Spike (S) protein (Figure 2(B)). Withanoside-IV had the docking score of  $-5.89$  Kcal/mol and in the best binding pose it was making hydrogen bond with the two residues Gln42 and Lys68 (Figure 2(C)). Further, 12-deoxywithastramonolide ( $-4.68$  Kcal/mol), Withaferin-A ( $-4.38$  Kcal/mol), Withanolide-A ( $-3.46$  Kcal/mol), Withanone ( $-3.27$  Kcal/mol), Withanolide-B ( $-3.18$  Kcal/mol) and methoxyWithaferin-A ( $-2.68$  Kcal/mol) also had a good binding score and were making at least one hydrogen bond in the best docking pose (Figure 2(D-H)). The docking conformations were re-assessed using AutoDock Vina, and it was found that most of the complexes had similar binding poses as generated by Glide. The docking score of all the complexes and the details of polar and nonpolar interactions are shown in Table 4. All the docked complexes were further subjected to classical MD of 100 ns to investigate the binding stability and crucial interactions between the ligands and protein. It was found in the MD trajectories that of all the ligands were interacting well with the ACE2 protein while Withanolide-A was deficient of a stable binding

during the simulation. Since all the other ligands were found to establish a stable contact with the protein, they were studied and analysed further. First, the RMSD calculation was done for all the simulated protein-ligand complexes and it was found that most of the complexes got stabilized within 20 ns of the simulation time without any significant fluctuations throughout the simulations thereafter (Figure 3(A)). However, a minor deviation peak was observed in Withanone between 40 and 60 ns of simulation, while after 60 ns all the complexes got converged. Among all the complexes, Withanolide-B ( $2.32 \pm 0.19$  Å) had the minimum deviation followed by Umifenovir ( $2.39 \pm 0.19$  Å), Withanoside-V ( $2.45 \pm 0.21$  Å), methoxyWithaferin-A ( $2.68 \pm 0.28$  Å), Withanoside-IV ( $2.74 \pm 0.39$  Å), 12-deoxywithastramonolide ( $2.85 \pm 0.38$  Å), Withanone ( $2.95 \pm 0.46$  Å) and Withaferin-A ( $3.05 \pm 0.38$  Å), respectively. Further, the complexes were analysed for the RMSF and it was found that all the complexes had the RMSF in the range of  $1.45 \pm 0.64$  Å, while only the loop region Phe320 to Lys340 had significant fluctuation of more than  $>3$  Å (Figure 3(B)). As the role of hydrogen bonding in providing affinity to drugs towards a receptor is well known, the hydrogen bond counts for the simulated trajectories were calculated. It was found that Withanoside-V ( $3.01 \pm 1.02$ ) had the highest number of average hydrogen bonds throughout the simulations, followed by Withanoside-IV ( $1.04 \pm 0.85$ ), Withanolide-B ( $0.98 \pm 0.44$ ), Withaferin-A ( $0.71 \pm 0.51$ ), methoxyWithaferin-A ( $0.66 \pm 0.58$ ), 12-deoxywithastramonolide ( $0.57 \pm 0.66$ ), Umifenovir ( $0.4 \pm 0.5$ ) and Withanone ( $0.08 \pm 0.30$ ), respectively (Figure 3(C)).

In order to explore the critical residues of ACE2 and their fraction of contacts with the ligands, the polar and nonpolar occupancy between the ligands and ACE2 were calculated. It was found that all the simulated ligands had numerous polar and nonpolar interactions at the binding site of ACE2. However, in terms of significant interactions ( $>30\%$  of the time of simulations) with critical residues (Ser19, Gln24, Lys34, Glu35, Asp38 and Gln42) of ACE2, which were involved in interaction with RBD of Spike protein, we found that Withanoside-V and Withanoside-IV were prominent among all the ligands, and even better than Umifenovir. Withanoside-V showed significant hydrogen bond interaction with Glu35, while Withanoside-IV with Glu35, Asp38 and Gln42 of ACE2 (Figure 4). Also, in order to investigate the binding affinity of the withanolides against ACE2, the MM/GBSA free binding energy calculations were performed. The results of MM/GBSA free binding energy showed that Withanoside-IV ( $-34.52 \pm 6.41$  Kcal/mol) had the highest affinity, followed by Withanone ( $-27.98 \pm 6.10$  Kcal/mol), 12-deoxywithastramonolide ( $-25.85 \pm 3.94$  Kcal/mol), methoxyWithaferin-A ( $-24.98 \pm 3.10$  Kcal/mol), Umifenovir ( $-22.12 \pm 3.54$  Kcal/mol), Withanoside-V ( $-21.22 \pm 4.67$  Kcal/mol), Withaferin-A ( $-20.69 \pm 7.64$  Kcal/mol) and Withanolide-B ( $-25.54 \pm 20.58$  Kcal/mol), respectively as shown in the plot (Figure 3(D)). The overall computational study suggested that Withanoside-IV and Withanoside-V were the best among all the withanolides, as

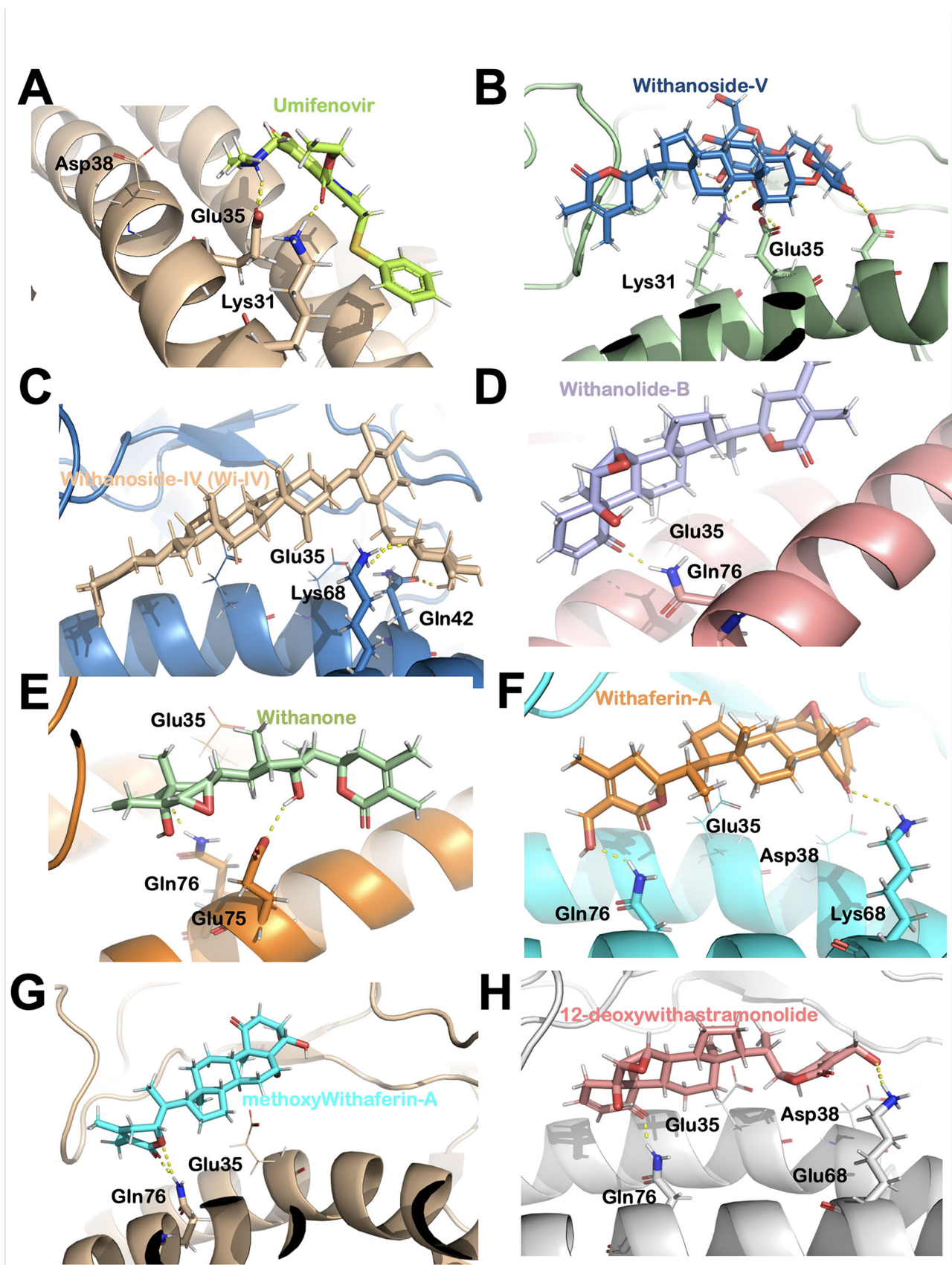


**Figure 2.** The best docked pose interactions between the ACE2 and the ligands, residues which are represented as stick showed the hydrogen bonding whereas residues shown as line are the crucial residues of ACE2 which were involved in hydrogen bonding with Spike protein but now making nonpolar interaction with the ligands (A) ACE2-Umifenovir (B) ACE2-Withanoside-V (C) ACE2-Withanoside-IV (D) ACE2- Withanolide-B (E) ACE2- Withanone (F) ACE2-Withaferin-A (G) ACE2-methoxyWithaferin-A (H) ACE2-12-deoxywithastramonolide.

**Table 4.** The molecular docking score and polar and nonpolar interactions in the best docking pose of ACE2-withanolides.

Complex	Molecular docking (Kcal/mol)	Types of interactions and residues involved ( Pre Molecular Dynamic Simulations)	
		H-bonds	Hydrophobic, polar and pi-pi stacking
ACE2–Umifenovir	–4.31	Lys31 Glu35	Asp38, Leu39, Phe72, Glu75, Gln76, Leu79
ACE2–Withanoside-V	–6.29	Lys31, Glu35, Asp38	Leu39, Phe72, Glu75, Leu79, Met82
ACE2–Withanoside-IV	–5.89	Gln42, Lys68	Phe28, Lys31, Glu35, Asp38, Leu39, Leu45, Ala46, Asn61, Ala65, Phe72, Glu75, Gln76, Leu79
ACE2–methoxyWithaferin-A	–2.68	Gln76	Phe28, Lys31, Glu35, Phe72, Glu75, Gln76, Leu79
ACE2–Withanolide-B	–3.18	Gln76	Phe28, Lys31, Glu35, Leu39, Lys68, Ala71, Phe72, Glu75, Leu79
ACE2–Withanolide-A	–3.46	Gln76	Phe28, Lys31, Glu35, Asp38, Leu39, Lys68, Phe72, Glu75, Leu79
ACE2–12-deoxywithastramonolide	–4.68	Lys68, Gln76	Phe28, Lys31, Glu35, Asp38, Leu39, Phe72, Glu75, Leu79
ACE2–Withaferin-A	–4.38	Lys68, Gln76	Phe28, Lys31, Glu35, Asp38, Leu39, Phe72, Glu75, Leu79
ACE2–Withanone	–3.27	Glu75, Gln76	Phe28, Lys31, Glu35, Leu39, Glu68, Ala71, Phe72, Leu79

well as Umifenovir to inhibit the interaction of ACE2 with SARS-CoV-2 Spike protein.

### 3.2. Cells treated with withanolides showed downregulation of ACE2 expression

We also prompted to evaluate the activities of these withanolides at subtoxic concentrations in cultured cells. We, firstly, screened the protein expression of ACE2 in various cancer cell lines (Supporting Information Figure S2) that led us to select three cell lines- HSC3 (oral squamous carcinoma cell line), A549 (non-small lung cancer cell line) and MCF-7 (human breast carcinoma cell line), given their moderate to low level of ACE2 expression. Cells treated with withanolides were subjected to mRNA and protein analysis. As shown in Figure 5(A), withanolides treated cells showed decrease in ACE2-mRNA and -protein expression. Of note, Withanone caused maximum decrease in ACE2 mRNA both in HSC3 and MCF7 cells. Withanolide A, Withanoside-IV and Withanoside-V also caused moderate decrease. Analysis of ACE2 protein levels in the withanolides treated cells also revealed significant decrease that was most prominent in Withanoside-IV and Withanoside-V treated cells (Figure 5(B)). In contrast to the decrease in ACE2 mRNA, ACE2 protein did not show decrease in Withanolide A-treated HSC3 cells. Conversely, MCF7 cells showed decrease in both in ACE2 mRNA and protein in withanolide-treated cells. Validation of protein levels by immunostaining (ICC) also showed an inhibitory activity of withanolides. Similar to the immunoblotting data, ICC showed decrease that was more prominent in MCF-7 cells (Figure 5(C,D)). Taken together, we found decrease in ACE2 expression in Withaferin-A, Withanone, Withanolide-A, Withanoside-IV and Withanoside-V in both the cell types; changes in mRNA were more prominent than the changes in protein (Figure 5).

We next validated the above results on malignant lung carcinoma (A549) cells and also investigated the effect of withanolides-rich aqueous extract from the well-segregated leaf (L) and stem (S) of Ashwagandha plant. We had earlier shown that the cyclic oligosaccharides *viz.* cyclodextrin could

augment extraction and stability of withanolides (Kaul et al., 2016) and were, therefore, used for withanolides enrichment in extraction. Given the fact that the content of withanolides is greater in leaves, while plant stem has more Withanone (Kaul et al., 2016; Kaur et al., 2018; Kumar, Dhanjal, Bhargava, et al., 2020), we enrolled subtoxic concentrations of both leaf and stem-based extracts prepared with cyclodextrins (soluble fraction- $\beta$ CD and insoluble fraction- $\beta$ DM). As shown in Figure 6(A,B), cells treated with three withanolides (Withaferin-A, Withanoside-IV, Withanoside-V) and withanolides-rich aqueous extracts from Ashwagandha stem (Ash M3- $\beta$ CD 27-S and Ash M3- $\beta$ DM 28-S) showed (10–20%) reduction in ACE2 expression both at the protein (as determined by immunoblotting) and mRNA (as determined by reverse transcription-polymerase chain reaction (RT-PCR)) levels. Conversely, immunostaining revealed reduction (~30% to 60%) in ACE2 protein in A549 cells treated with different withanolides (Withaferin, Withanone, Withanolide-A, Withanoside-IV, Withanoside-V) and in withanolides-rich extracts (Figure 6(C)). These data revealed that the withanolides/extracts may inhibit the virus infection by multiple ways including (i) inhibition of virus entry to the cells by blocking its interaction with ACE2-host cell surface receptor and (ii) reduction in the level of expression of ACE2 mRNA and protein.

## 4. Discussion

ACE2, a host receptor, plays an important role in the first step of the viral infection. The attachment of RBD of SARS-CoV-2 S protein to the host ACE2 is the crucial step for the virus entry into the host cell (Casella et al., 2020; Hoffmann et al., 2020). It has been shown in previous studies that SARS-CoV-2 could not infect the cells that were not expressing the ACE2 protein (Lan et al., 2020). The previously reported coronaviruses such as SARS-CoV and MERS also had the similar mechanism of entry through ACE2. However, the binding affinity, hence the higher infectivity rate, of SARS-CoV-2 is found to be 10- to 20-fold higher (Nguyen et al., 2020). Targeting ACE2 could thus lead to inhibition or reduction of viral infection. Given the severity of the COVID-19

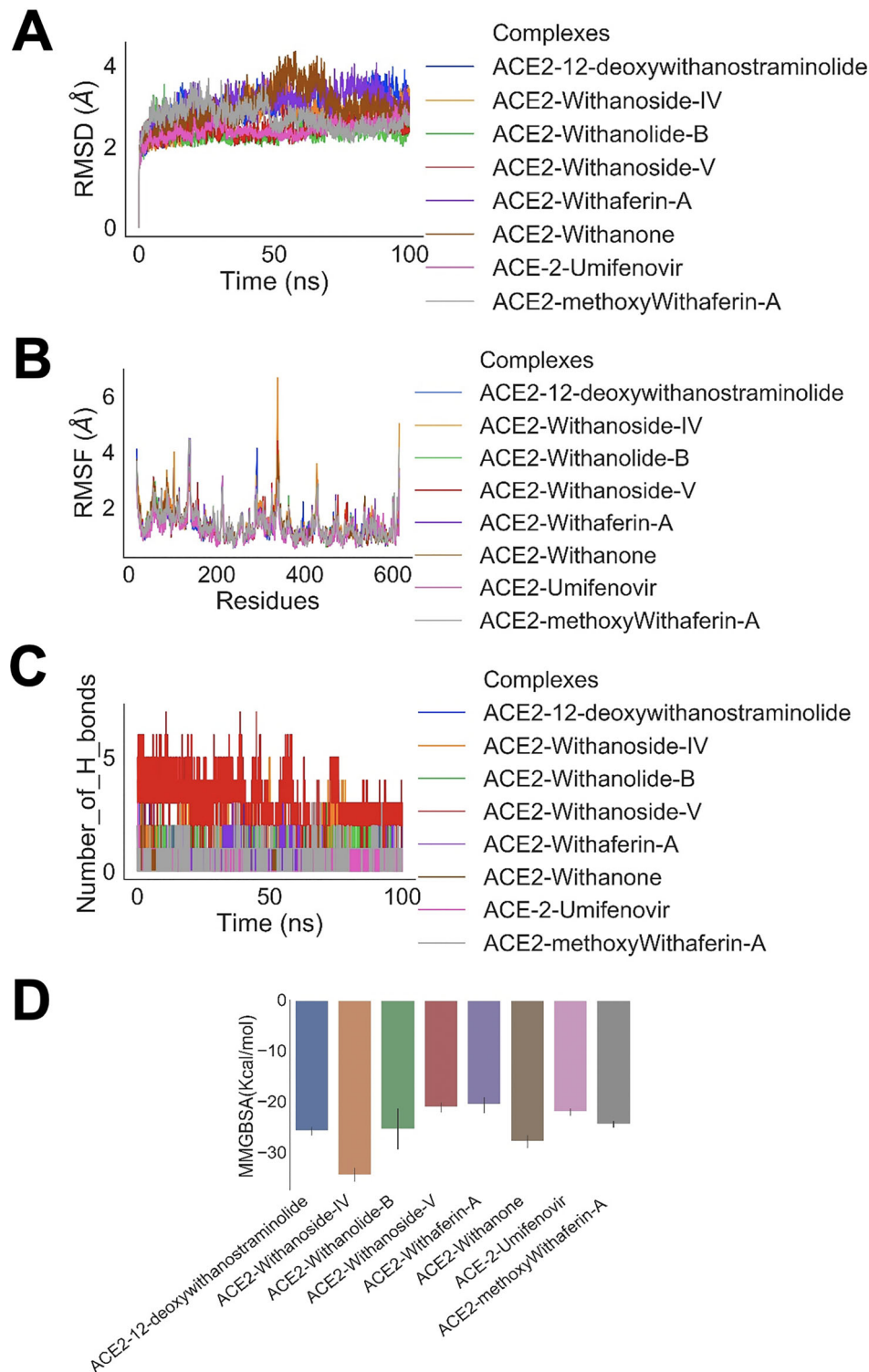


**Figure 3.** The MD analysis of the simulated systems (A) The RMSD plot of the ACE2–ligand complexes showing the stable trajectories throughout the duration of simulation (B) The RMSF plot shows the stable protein–ligand complexes, while loop region from Phe320 to Lys340 has significant fluctuation. (C) The hydrogen bond count plot of the ACE2–ligands, shows Withanoside-V and Withanoside-IV have significant hydrogen bonding throughout the simulation (D) The plot of the MM/GBSA free binding energy for the 100 frames extracted from 40 to 100 ns of the simulations at an interval of 30 frames indicated that Withanoside-IV had the highest and consistent binding energy followed by Withanone, methoxyWithaferin-A and 12-deoxywithastraminolide, respectively.

pandemic, the quicker and safer way of drug discovery is drug repurposing against ACE2 for anti-COVID-19 activity. There are various FDA approved drugs which are in advanced stages of clinical trials against SARS-CoV-2 such as lopinavir, remdesivir, ribavirin, arbidol (umifenovir), camostat

mesylate, hydroxychloroquine and many more (Drożdżal et al., 2020; McKee et al., 2020). Specifically, arbidol an influenza A virus fusion inhibitor was found to be effective in the preliminary studies against ACE2-S protein interaction inhibition (Jin et al., 2020; Kadam & Wilson, 2017). In another



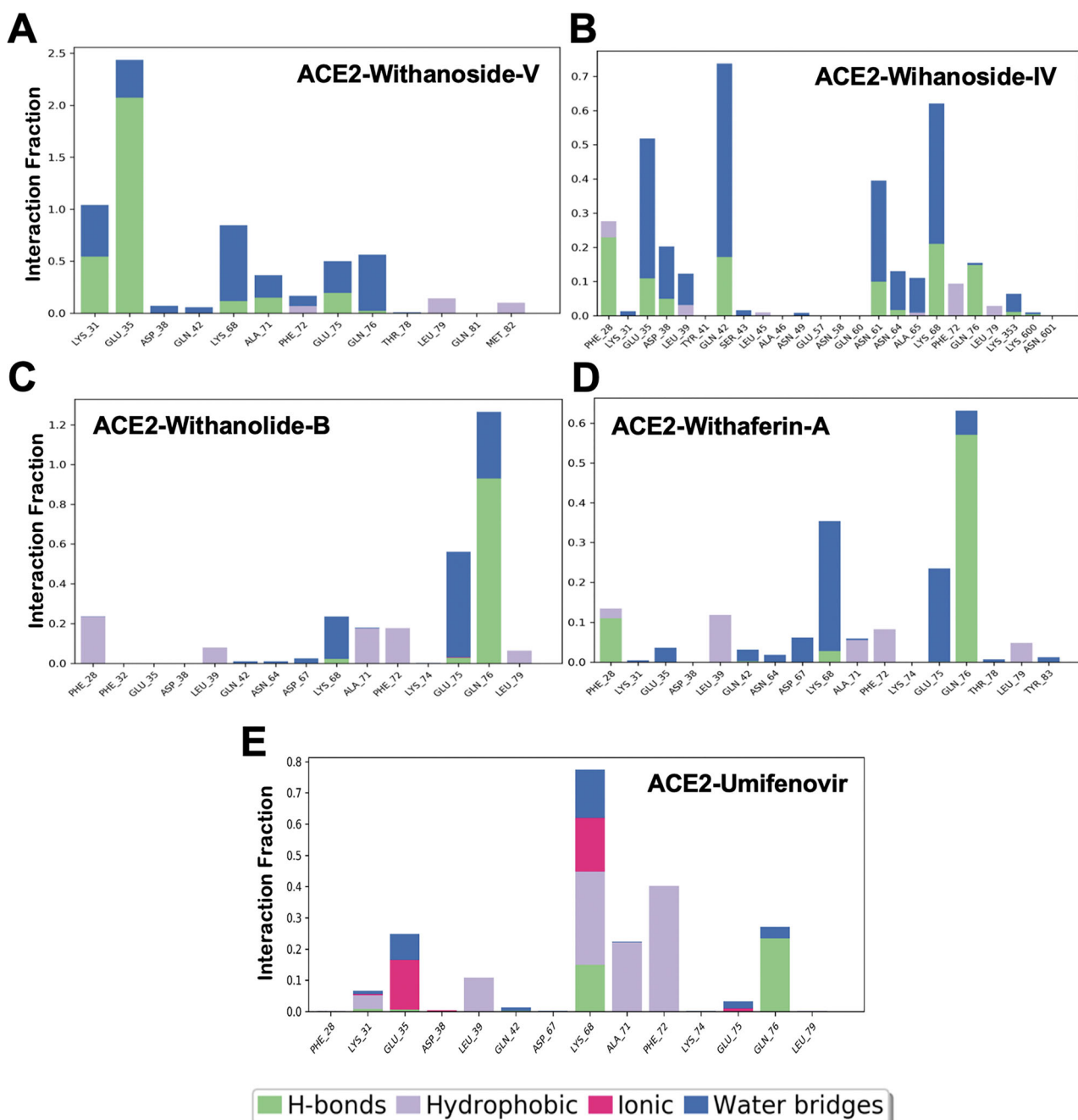


**Figure 4.** The best four ACE2-ligand complexes having the significant interaction occupancies. (A) ACE2-Withanoside-V, (B) ACE2-Withanoside-IV, (C) Withanolide-B, (D) Withaferin-A, (E) Umifenovir.

study using modeled surface and living cells, it has been demonstrated that N-terminal ACE2 mimicking peptide could be the potent inhibitor of S protein-ACE2 interactions (Clausen et al., 2020). There are various approved antimicrobial agents such as ciclopirox, dolutegravir, trotrazuril and enalapril maleate having  $AC_{50}$  less 8 micromoles that are found to be effective in interfering with the interaction of ACE2-S protein using cell-based assays (Hanson et al., 2020). Other affordable and safer alternatives to the synthetic drugs are natural metabolites from the plant sources. Many studies on plant-based compound screening against SARS-CoV-2 and many alkaloids, flavonoids and terpenoids molecules have been recently reported as potential drug candidates against ACE2 (Muhseen et al., 2020; Russo et al., 2020). Among all

the natural compounds, withanolides from Ashwagandha has been shown to be very promising in preliminary studies against SARS-CoV-2 (Chikhale et al., 2020; Shree et al., 2020; Straughn & Kakar, 2020). Ashwagandha is being used in traditional home medicine in India and has been shown to possess a variety of bioactivities mainly against oxidative stress, brain disorders, cancers, microbial infections and immune response (Mishra et al., 2000; Singh et al., 2011). Recent COVID-19 studies have suggested that the viral infection can enhance the immune response and thus can lead to cytokine storm that could be fatal to the patients. In various studies, it has been shown that Withaferin-A can reduce the secretion of various cytokines such as TNFs and interleukins (Dubey et al., 2018; Straughn & Kakar, 2019). It has also been

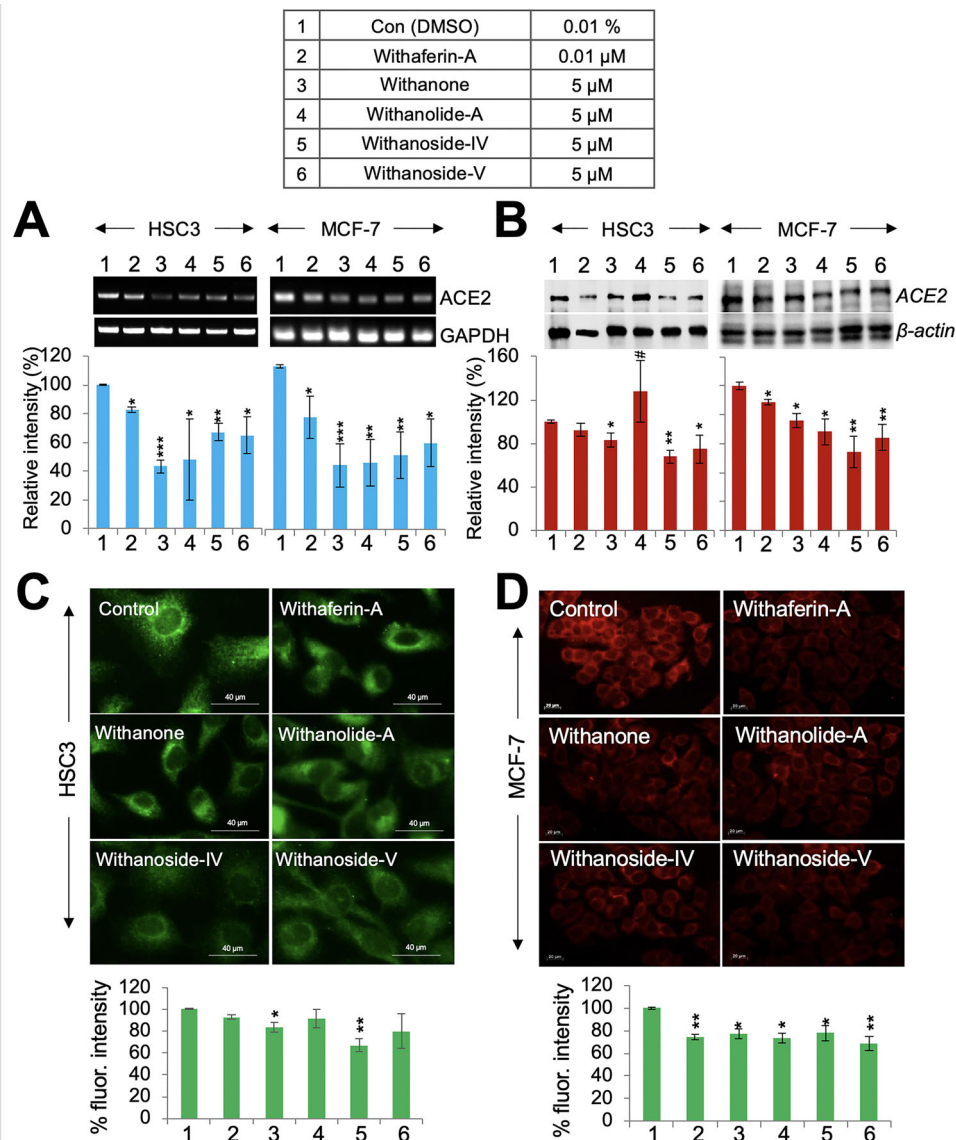


**Figure 5.** Biochemical analyses of withanolides activity on ACE2 in HSC3 and MCF-7 cells. (A) Semi-quantitative RT-PCR showing ACE2 expression in withanolides treated HSC3 and MCF-7 cells, quantitation is shown below. (B) Immunoblots showing ACE2 transcript levels in withanolides treated HSC3 and MCF-7 cells, quantitation is shown below. Immunostaining showing ACE2 expression in withanolides treated HSC3 (C) and MCF-7 (D) cells, quantitation is shown below.

recently reported that Withanone could be an effective inhibitor of ACE2 (Balkrishna et al., 2020). Our group has also recently reported the potential inhibitory action of Withanone and Withaferin-A against Main protease of SARS-CoV-2 and host cell receptor TMPRSS2 through computational and experimental assays (Kumar, Dhanjal, Bhargava, et al., 2020; Kumar, Dhanjal, Kaul, et al., 2020). The Ashwagandha-derived withanolides have also been shown to possess anti-viral activities against influenza and herpes simplex viruses (Cai et al., 2015; Grover et al., 2011). Computational analysis involved molecular docking, classical MD simulations, binding free energy calculations and experimental assays to investigate the activity of withanolides against ACE2 receptor. This was carried out to understand the potential of withanolides to inhibit the interaction between host ACE2 and S protein of SARS-CoV-2. In the original crystal structure of ACE2, Ser19, Gln24, Lys34, Glu35, Asp38 and Gln42 of ACE2 were making contact with RBD of

S protein. Hence, we probed the potential of the withanolides to bind at the ACE2-S protein receptor surface and inhibit the crucial interactions between them. Through the molecular docking and MD simulations, it was found that Withanoside-V was able to interact with Glu35, while Withanoside-IV interacted with Glu35, Asp38 and Gln 42 of ACE2. Out of eight withanolides studied, the MM/GBSA binding free energy calculations were the best for Withanoside-IV and -V predicting their high potential as novel inhibitor candidates. Effect of these withanolides on ACE2 expression level was investigated using human oral (HSC3), lung (A549) and breast (MCF-7) cancer cells. Oral and lung cavity epithelium is the primary site of SARS-CoV-2 infection, therefore enrolment of HSC3 and A549 cells provided a comprehensive *in vitro* system to test ACE2-inhibitory activity of withanolides and withanolides-rich Ashwagandha leaf and stem extracts. The cells treated with withanolides as well as extracts showed reduction in ACE2 expression, although to a variable

1	Con (DMSO)	0.01 %
2	Withaferin-A	0.01 $\mu$ M
3	Withanone	5 $\mu$ M
4	Withanolide-A	5 $\mu$ M
5	Withanoside-IV	5 $\mu$ M
6	Withanoside-V	5 $\mu$ M
7	Ash M2H1- $\beta$ CD 23-L	-
8	Ash M2H1- $\beta$ DM 24-L	-
9	Ash M3- $\beta$ CD 27-S	-
10	Ash M3- $\beta$ DM 28-S	-

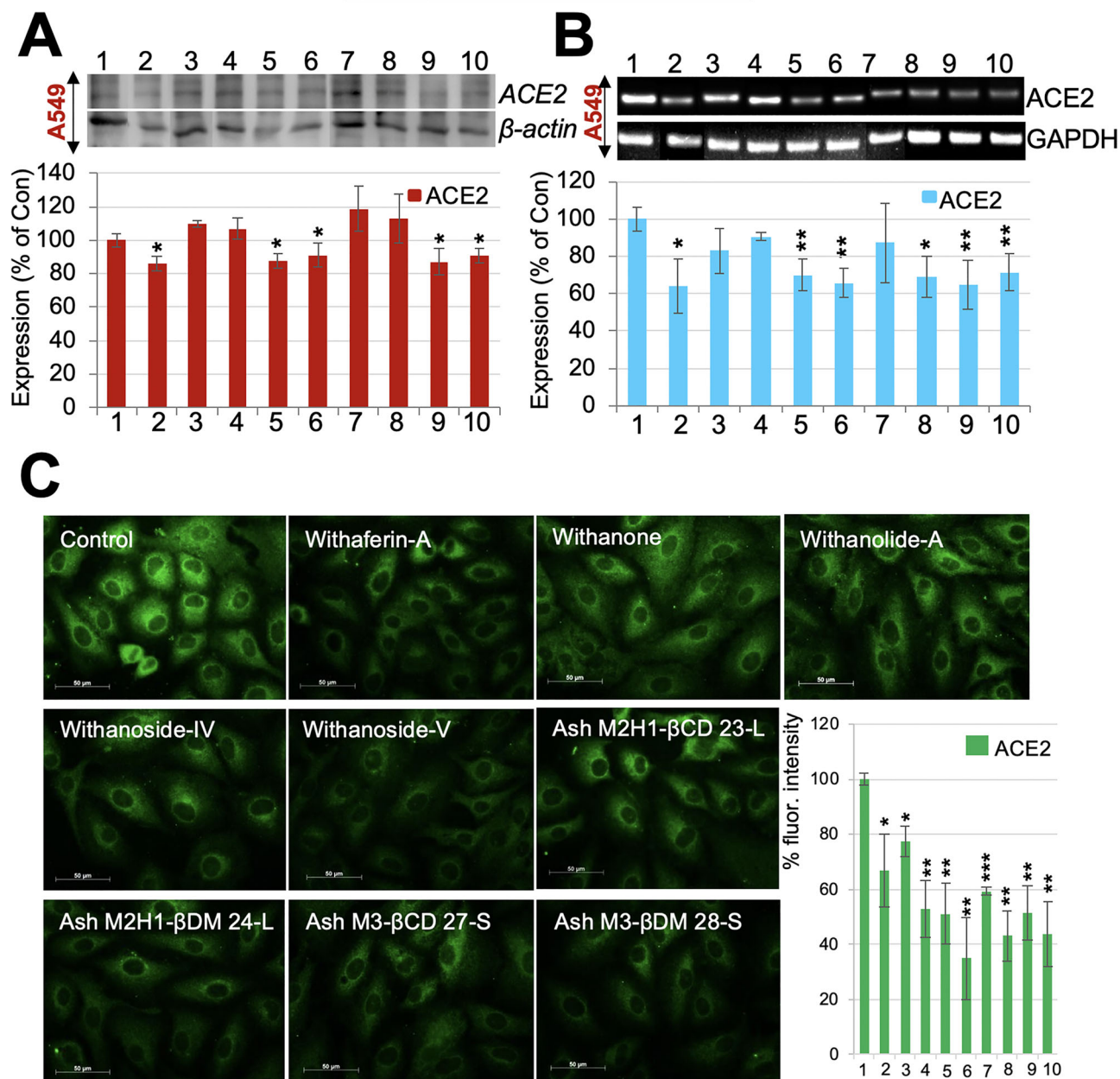


**Figure 6.** Biochemical analysis of activities of withanolides and Ashwagandha extracts on ACE2. (A) Immunoblots showing ACE2 expression in withanolides- and Ashwagandha extracts-treated A549 cells; quantitation is shown below. (B) Semi-quantitative RT-PCR showing ACE2 transcript levels in withanolides- and Ashwagandha extracts-treated A549 cells. Quantitation is shown at the right. (C) Immunostaining showing ACE2 expression in withanolides- and Ashwagandha extracts-treated A549 cells. The quantitation is shown at the right.

extent in different cell types, both at the protein and mRNA level.

Medicinal value of Ashwagandha has been attributed to have anti-stress and health benefiting effects (Chaudhary et al., 2017). Multiple reports previously have underlined potential of Ashwagandha for inducing tumor-suppressor activity and anti-inflammatory activities (Bhargava et al., 2019; Chaudhary et al., 2017; Gao et al., 2014; Grover, Priyandoko, et al., 2012; Grover, Singh, et al., 2012; Sundar et al., 2019; Widodo et al., 2007, 2010; Yu et al., 2017). Ashwagandha withanolides were also studied for their anti-viral effects, wherein Withaferin-A was shown to be effective against herpes simplex virus, HIV and H1N1 influenza virus (Cai et al., 2015; Grover et al., 2011; Shi et al., 2017). Aqueous extracts of Ashwagandha leaf and stem provide affordable and readily accessible withanolides-rich alternative of purified withanolides, which made it a promising resource for usage for a variety of health benefits facilitated by its multimodal action. ACE2 inhibitory activity of stem-based cyclodextrins ( $\beta$ CD and  $\beta$ DM) extracts may offer a holistic remedial approach for management of COVID-19. Applications of these withanolides-rich extracts could be examined further to ensure their clinical outcome and a possible accumulative health-benefits. We have recently reported the antagonizing potential of Withanone on TMPRSS2 (Kumar, Dhanjal, Bhargava, et al., 2020). Moreover, it was also predicted to target the main protease ( $M^{pro}$ ) of SARS-CoV-2 that is essential for its replication in host cells (Kumar, Dhanjal, Kaul, et al., 2020). Here, we further identified ACE2-inhibiting activities of Ashwagandha withanolides and its withanolides-rich extracts using computational and *in vitro* assays comprising oral, lung and breast cancer cells. In a recent study, purified Ashwagandha extract having 35% of glycowithanolides (Withanoside-IV and Withanoside-V) was used to study acute and sub chronic toxicity in rats. The repeated administration of the extract for 90 days in rats at the maximum dose level of 1000 mg/kg body weight did not induce any observable toxic effects when compared to its corresponding control animals. No mortality or clinical signs of toxicity were observed in any of the animals at maximum recommended dose level of 2000 mg/kg (Antony et al., 2018). In this study, we demonstrated that among the 8 tested withanolides, Withaferin-A, Withanone, Withanoside-IV, Withanoside-V possessed an ACE2 inhibitory activity. Besides these, withanolides as well as the water-based extracts from Ashwagandha caused inhibition of ACE2 expression and hence are suggested to be tested further to offer useful resource for COVID-19 therapeutics and drug development.

## Disclosure statement

No potential conflict of interest was reported by the authors.

## Funding

This study was supported by the funds granted by AIST (Japan) and DBT (Government of India).

## Author's contributions

Conceptualization - R.S.K., V.K., D.S., R.W.; Bioinformatics work and formal analysis- V.K., J.K.D., D.S.; Experimental work - R.S.K., J.K.D., S.G., X.L.; Funding acquisition - S.C.K., R.W., D.S.; Writing - review & editing R.S.K., V.K., J.K.D., S. G., S.C.K., R.W., D.S. All authors contributed to the development of this manuscript and read and approved the final version.

## Availability of data and materials

All data generated or analyzed during this study are included in this published article.

## References

- Ali, A., & Vijayan, R. (2020). Dynamics of the ACE2-SARS-CoV-2/SARS-CoV spike protein interface reveal unique mechanisms. *Scientific Reports*, 10(1), 14214. <https://doi.org/10.1038/s41598-020-71188-3>
- Antony, B., Benny, M., Kuruvilla, B. T., Gupta, N. K., Sebastian, A., & Jacob, S. (2018). ACUTE AND SUB CHRONIC TOXICITY STUDIES OF PURIFIED WITHANIA SOMNIFERA EXTRACT IN RATS. *International Journal of Pharmacy and Pharmaceutical Sciences*, 10(12), 41–46. <https://doi.org/10.22159/ijpps.2018v10i12.29493>
- Balkrishna, A., Pokhrel, S., Singh, J., & Varshney, A. (2020). Withanone from *Withania somnifera* may inhibit novel Coronavirus (COVID-19) entry by disrupting interactions between viral S-protein receptor binding domain and host ACE2 receptor. PREPRINT (Version 1) available at Research Square. <https://www.researchsquare.com/article/rs-17806/v1>
- Bhargava, P., Malik, V., Liu, Y., Ryu, J., Kaul, S. C., Sundar, D., & Wadhwa, R. (2019). Molecular insights into withaferin-A-induced senescence: Bioinformatics and experimental evidence to the role of NF $\kappa$ B and CARF. *The Journals of Gerontology. Series A, Biological Sciences and Medical Sciences*, 74(2), 183–191. <https://doi.org/10.1093/geronol/gly107>
- Cai, Z., Zhang, G., Tang, B., Liu, Y., Fu, X., & Zhang, X. (2015). Promising anti-influenza properties of active constituent of *Withania somnifera* ayurvedic herb in targeting neuraminidase of H1N1 influenza: Computational study. *Cell Biochemistry and Biophysics*, 72(3), 727–739. <https://doi.org/10.1007/s12013-015-0524-9>
- Cascella, M., Rajnik, M., Cuomo, A., Dulebohn, S. C., Di Napoli, R. (2020). Features, evaluation and treatment coronavirus (COVID-19) (*StatPearls*). <http://www.ncbi.nlm.nih.gov/pubmed/32150360>
- Chaudhary, A., Kalra, R. S., Huang, C., Prakash, J., Kaul, S. C., & Wadhwa, R. (2017). 2,3-Dihydro-3 $\beta$ -methoxy withaferin-a protects normal cells against stress: Molecular evidence of its potent cytoprotective activity. *Journal of Natural Products*, 80(10), 2756–2760. <https://doi.org/10.1021/acs.jnatprod.7b00573>
- Chaudhary, A., Kalra, R. S., Malik, V., Katiyar, S. P., Sundar, D., Kaul, S. C., & Wadhwa, R. (2019). 2, 3-dihydro-3 $\beta$ -methoxy withaferin-A lacks anti-metastasis potency: Bioinformatics and experimental evidences. *Scientific Reports*, 9(1), 17344. <https://doi.org/10.1038/s41598-019-53568-6>
- Chikhale, R. V., Gurav, S. S., Patil, R. B., Sinha, S. K., Prasad, S. K., Shalkya, A., Shrivastava, S. K., Gurav, N. S., & Prasad, R. S. (2020). Sars-cov-2 host entry and replication inhibitors from Indian ginseng: An in-silico approach. *Journal of Biomolecular Structure and Dynamics*, 1–12. <https://doi.org/10.1080/07391102.2020.1778539>
- Choudhary, S., & Silakari, O. (2020). Scaffold morphing of arbidol (umifenovir) in search of multi-targeting therapy halting the interaction of SARS-CoV-2 with ACE2 and other proteases involved in COVID-19. *Virus Research*, 289, 198146. <https://doi.org/10.1016/j.virusres.2020.198146>
- Clausen, T. M., Sandoval, D. R., Spliid, C. B., Pihl, J., Perrett, H. R., Painter, C. D., Narayanan, A., Majowicz, S. A., Kwong, E. M., McVicar, R. N., Thacker, B. E., Glass, C. A., Yang, Z., Torres, J. L., Golden, G. J., Bartels, P. L., Porell, R. N., Garretson, A. F., Laubach, L., ... Esko, J. D. (2020).

- SARS-CoV-2 infection depends on cellular heparan sulfate and ACE2. *Cell*, 183(4), 1043–1057. <https://doi.org/10.1016/j.cell.2020.09.033>
- Donoghue, M., Hsieh, F., Baronas, E., Godbout, K., Gosselin, M., Stagliano, N., Donovan, M., Woolf, B., Robison, K., Jeyaseelan, R., Breitbart, R. E., & Acton, S. (2000). A novel angiotensin-converting enzyme-related carboxypeptidase (ACE2) converts angiotensin I to angiotensin 1-9. *Circulation Research*, 87(5), E1–E9. <https://doi.org/10.1161/01.res.87.5.e1>
- Drożdżal, S., Rosik, J., Lechowicz, K., Machaj, F., Kótfis, K., Ghavami, S., & Łos, M. J. (2020). FDA approved drugs with pharmacotherapeutic potential for SARS-CoV-2 (COVID-19) therapy. *Drug Resistance Updates: Reviews and Commentaries in Antimicrobial and Anticancer Chemotherapy*, 53, 100719. <https://doi.org/10.1016/j.drug.2020.100719>
- Dubey, S., Yoon, H., Cohen, M. S., Nagarkatti, P., Nagarkatti, M., & Karan, D. (2018). Withaferin A associated differential regulation of inflammatory cytokines. *Frontiers in Immunology*, 9, 195. <https://doi.org/10.3389/fimmu.2018.00195>
- Friesner, R. A., Murphy, R. B., Repasky, M. P., Frye, L. L., Greenwood, J. R., Halgren, T. A., Sanschagrin, P. C., & Mainz, D. T. (2006). Extra precision glide: Docking and scoring incorporating a model of hydrophobic enclosure for protein–ligand complexes. *Journal of Medicinal Chemistry*, 49(21), 6177–6196. <https://doi.org/10.1021/jm051256o>
- Gao, R., Shah, N., Lee, J. S., Katiyar, S. P., Li, L., Oh, E., Sundar, D., Yun, C. O., Wadhwa, R., & Kaul, S. C. (2014). Withanone-rich combination of Ashwagandha withanolides restricts metastasis and angiogenesis through hnRNP-K. *Molecular Cancer Therapeutics*, 13(12), 2930–2940. <https://doi.org/10.1158/1535-7163.MCT-14-0324>
- Grover, A., Agrawal, V., Shandilya, A., Bisaria, V. S., & Sundar, D. (2011). Non-nucleosidic inhibition of Herpes simplex virus DNA polymerase: Mechanistic insights into the anti-herpetic mode of action of herbal drug withaferin A. *BMC Bioinformatics*, 12 (Suppl 13), S22. <https://doi.org/10.1186/1471-2105-12-S13-S22>
- Grover, A., Priyandoko, D., Gao, R., Shandilya, A., Widodo, N., Bisaria, V. S., Kaul, S. C., Wadhwa, R., & Sundar, D. (2012). Withanone binds to mortalin and abrogates mortalin-p53 complex: Computational and experimental evidence. *The International Journal of Biochemistry & Cell Biology*, 44(3), 496–504. <https://doi.org/10.1016/j.biocel.2011.11.021>
- Grover, A., Singh, R., Shandilya, A., Priyandoko, D., Agrawal, V., Bisaria, V. S., Wadhwa, R., Kaul, S. C., & Sundar, D. (2012). Ashwagandha derived withanone targets TPX2-Aurora A complex: Computational and experimental evidence to its anticancer activity. *PLoS One*, 7(1), e30890. <https://doi.org/10.1371/journal.pone.0030890>
- Hanson, Q. M., Wilson, K. M., Shen, M., Itkin, Z., Eastman, R. T., Shinn, P., & Hall, M. D. (2020). Targeting ACE2-RBD interaction as a platform for COVID19 therapeutics: Development and drug repurposing screen of an AlphaLISA proximity assay. *bioRxiv*. <https://doi.org/10.1101/2020.06.16.154708>. *ACS Pharmacology & Translational Science*, 3(6), 1352–1360. <https://doi.org/10.1021/acscptsci.0c00161>
- Harder, E., Damm, W., Maple, J., Wu, C., Reboul, M., Xiang, J. Y., Wang, L., Lupyán, D., Dahlgren, M. K., Knight, J. L., Kaus, J. W., Cerutti, D. S., Krilov, G., Jorgensen, W. L., Abel, R., & Friesner, R. A. (2016). OPLS3: A force field providing broad coverage of drug-like small molecules and proteins. *Journal of Chemical Theory and Computation*, 12(1), 281–296. <https://doi.org/10.1021/acs.jctc.5b00864>
- Hoffmann, M., Kleine-Weber, H., Schroeder, S., Kruger, N., Herrler, T., Erichsen, S., Schiergens, T. S., Herrler, G., Wu, N. H., Nitsche, A., Müller, M. A., Drosten, C., & Pohlmann, S. (2020). SARS-CoV-2 cell entry depends on ACE2 and TMPRSS2 and is blocked by a clinically proven protease inhibitor. *Cell*, 181(2), 271–280. <https://doi.org/10.1016/j.cell.2020.02.052>
- Hulswit, R. J., de Haan, C. A., & Bosch, B. J. (2016). Coronavirus spike protein and prism changes. *Advances in Virus Research*, 96, 29–57. <https://doi.org/10.1016/bs.aivir.2016.08.004>
- Jin, Z., Du, X., Xu, Y., Deng, Y., Liu, M., Zhao, Y., Zhang, B., Li, X., Zhang, L., Peng, C., Duan, Y., Yu, J., Wang, L., Yang, K., Liu, F., Jiang, R., Yang, X., You, T., Liu, X., ... Yang, H. (2020). Structure of Mpro from SARS-CoV-2 and discovery of its inhibitors. *Nature*, 582(7811), 289–293. <https://doi.org/10.1038/s41586-020-2223-y>
- Kadam, R. U., & Wilson, I. A. (2017). Structural basis of influenza virus fusion inhibition by the antiviral drug Arbidol. *Proceedings of the National Academy of Sciences of the United States of America*, 114(2), 206–214. <https://doi.org/10.1073/pnas.1617020114>
- Kalra, R. S., & Kandimalla, R. (2021). Engaging the spikes: Heparan sulfate facilitates SARS-CoV-2 spike protein binding to ACE2 and potentiates viral infection. *Signal Transduction and Targeted Therapy*, 6(1), 39. <https://doi.org/10.1038/s41392-021-00470-1>
- Kalra, R. S., Tomar, D., Meena, A. S., & Kandimalla, R. (2020). SARS-CoV-2, ACE2, and hydroxychloroquine: Cardiovascular complications, therapeutics, and clinical readouts in the current settings. *Pathogens*, 9(7), 546. <https://doi.org/10.3390/pathogens9070546>
- Kaul, S. C., Ishida, Y., Tamura, K., Wada, T., Iitsuka, T., Garg, S., Kim, M., Gao, R., Nakai, S., Okamoto, Y., Terao, K., & Wadhwa, R. (2016). Novel methods to generate active ingredients-enriched Ashwagandha leaves and extracts. *PLoS One*, 11(12), e0166945. <https://doi.org/10.1371/journal.pone.0166945>
- Kaur, A., Singh, B., Ohri, P., Wang, J., Wadhwa, R., Kaul, S. C., Pati, P. K., & Kaur, A. (2018). Organic cultivation of Ashwagandha with improved biomass and high content of active withanolides: Use of Vermicompost. *PLoS One*, 13(4), e0194314. <https://doi.org/10.1371/journal.pone.0194314>
- Kumar, S. (2020). Drug and vaccine design against Novel Coronavirus (2019-nCoV) spike protein through Computational approach. *Preprints (2020020071)*. <https://doi.org/10.20944/preprints202002.0071.v1>
- Kumar, V., Dhanjal, J. K., Bhargava, P., Kaul, A., Wang, J., Zhang, H., Kaul, S. C., Wadhwa, R., & Sundar, D. (2020). Withanone and Withaferin-A are predicted to interact with transmembrane protease serine 2 (TMPRSS2) and block entry of SARS-CoV-2 into cells. *Journal of Biomolecular Structure and Dynamics*, 1–13. <https://doi.org/10.1080/07391102.2020.1775704>
- Kumar, V., Dhanjal, J. K., Kaul, S. C., Wadhwa, R., & Sundar, D. (2020). Withanone and caffeic acid phenethyl ester are predicted to interact with main protease (M(pro)) of SARS-CoV-2 and inhibit its activity. *Journal of Biomolecular Structure and Dynamics*, 1–13. <https://doi.org/10.1080/07391102.2020.1772108>
- Lan, J., Ge, J., Yu, J., Shan, S., Zhou, H., Fan, S., Zhang, Q., Shi, X., Wang, Q., Zhang, L., & Wang, X. (2020). Structure of the SARS-CoV-2 spike receptor-binding domain bound to the ACE2 receptor. *Nature*, 581(7807), 215–220. <https://doi.org/10.1038/s41586-020-2180-5>
- Letko, M., Marzi, A., & Munster, V. (2020). Functional assessment of cell entry and receptor usage for SARS-CoV-2 and other lineage B betacoronaviruses. *Nature Microbiology*, 5(4), 562–569. <https://doi.org/10.1038/s41564-020-0688-y>
- Li, F. (2008). Structural analysis of major species barriers between humans and palm civets for severe acute respiratory syndrome coronavirus infections. *Journal of Virology*, 82(14), 6984–6991. <https://doi.org/10.1128/JVI.00442-08>
- Li, F., Li, W., Farzan, M., & Harrison, S. C. (2005). Structure of SARS coronavirus spike receptor-binding domain complexed with receptor. *Science (New York, N.Y.)*, 309(5742), 1864–1868. <https://doi.org/10.1126/science.1116480>
- Li, M. Y., Li, L., Zhang, Y., & Wang, X. S. (2020). Expression of the SARS-CoV-2 cell receptor gene ACE2 in a wide variety of human tissues. *Infectious Diseases of Poverty*, 9(1), 45. <https://doi.org/10.1186/s40249-020-00662-x>
- Lu, R., Zhao, X., Li, J., Niu, P., Yang, B., Wu, H., Wang, W., Song, H., Huang, B., Zhu, N., Bi, Y., Ma, X., Zhan, F., Wang, L., Hu, T., Zhou, H., Hu, Z., Zhou, W., Zhao, L., ... Tan, W. (2020). Genomic characterisation and epidemiology of 2019 novel coronavirus: Implications for virus origins and receptor binding. *Lancet (London, England)*, 395(10224), 565–574. [https://doi.org/10.1016/S0140-6736\(20\)30251-8](https://doi.org/10.1016/S0140-6736(20)30251-8)
- Madhavi Sastry, G., Adzhigirey, M., Day, T., Annabhimoju, R., & Sherman, W. (2013). Protein and ligand preparation: Parameters, protocols, and influence on virtual screening enrichments. *Journal of Computer-Aided Molecular Design*, 27(3), 221–234. <https://doi.org/10.1007/s10822-013-9644-8>
- McKee, D. L., Sternberg, A., Stange, U., Laufer, S., & Naujokat, C. (2020). Candidate drugs against SARS-CoV-2 and COVID-19. *Pharmacological Research*, 157, 104859. <https://doi.org/10.1016/j.phrs.2020.104859>

- Mishra, L. C., Singh, B. B., & Dagenais, S. (2000). Scientific basis for the therapeutic use of *Withania somnifera* (Ashwagandha): A review. *Alternative Medicine Review: A Journal of Clinical Therapeutic*, 5(4), 334–346.
- Muhseen, Z. T., Hameed, A. R., Al-Hasani, H. M. H., Tahir UI Qamar, M., & Li, G. (2020). Promising terpenes as SARS-CoV-2 spike receptor-binding domain (RBD) attachment inhibitors to the human ACE2 receptor: Integrated computational approach. *Journal of Molecular Liquids*, 320, 114493. <https://doi.org/10.1016/j.molliq.2020.114493>
- Nguyen, H. L., Lan, P. D., Thai, N. Q., Nissley, D. A., O'Brien, E. P., & Li, M. S. (2020). Does SARS-CoV-2 bind to human ACE2 more strongly than does SARS-CoV? *The Journal of Physical Chemistry B*, 124(34), 7336–7347. <https://doi.org/10.1021/acs.jpcc.0c04511>
- Padhi, A. K., Seal, A., Khan, J. M., Ahamed, M., & Tripathi, T. (2021). Unraveling the mechanism of arbidol binding and inhibition of SARS-CoV-2: Insights from atomistic simulations. *European Journal of Pharmacology*, 894, 173836. <https://doi.org/10.1016/j.ejphar.2020.173836>
- Pagadala, N. S., Syed, K., & Tuszyński, J. (2017). Software for molecular docking: A review. *Biophysical Reviews*, 9(2), 91–102. <https://doi.org/10.1007/s12551-016-0247-1>
- Rota, P. A., Oberste, M. S., Monroe, S. S., Nix, W. A., Campagnoli, R., Icenogle, J. P., Penaranda, S., Bankamp, B., Maher, K., Chen, M. H., Tong, S., Tamin, A., Lowe, L., Frace, M., DeRisi, J. L., Chen, Q., Wang, D., Erdman, D. D., Peret, T. C., ... Bellini, W. J. (2003). Characterization of a novel coronavirus associated with severe acute respiratory syndrome. *Science (New York, N.Y.)*, 300(5624), 1394–1399. <https://doi.org/10.1126/science.1085952>
- Russo, M., Moccia, S., Spagnuolo, C., Tedesco, I., & Russo, G. L. (2020). Roles of flavonoids against coronavirus infection. *Chemico-Biological Interactions*, 328, 109211. <https://doi.org/10.1016/j.cbi.2020.109211>
- Schrödinger. (2020). Glide, ligprep, protein preparation wizard, prime, desmond molecular dynamics system. Maestro-Desmond Interoperability Tools Schrödinger, LLC.
- Shi, T., Wilhelm, E., Bell, B., & Dumais, N. (2017). Nf- $\kappa$ b-dependent inhibition of HIV-1 transcription by withaferin A. *HIV: Current Research*, 02(01), 2572. <https://doi.org/10.4172/2572-0805.1000119>
- Shree, P., Mishra, P., Selvaraj, C., Singh, S. K., Chaube, R., Garg, N., & Tripathi, Y. B. (2020). Targeting COVID-19 (SARS-CoV-2) main protease through active phytochemicals of ayurvedic medicinal plants - *Withania somnifera* (Ashwagandha), *Tinospora cordifolia* (Giloy) and *Ocimum sanctum* (Tulsi) - A molecular docking study. *Journal of Biomolecular Structure and Dynamics*, 1–14. <https://doi.org/10.1080/07391102.2020.1810778>
- Singh, N., Bhalla, M., de Jager, P., & Gilca, M. (2011). An overview on Ashwagandha: A Rasayana (rejuvenator) of Ayurveda. *African Journal of Traditional, Complementary and Alternative Medicines*, 8(5 Suppl), 208–213. <https://doi.org/10.4314/ajtcam.v8i5S.9>
- Straughn, A. R., & Kakar, S. S. (2019). Withaferin A ameliorates ovarian cancer-induced cachexia and proinflammatory signaling. *Journal of Ovarian Research*, 12(1), 115. <https://doi.org/10.1186/s13048-019-0586-1>
- Straughn, A. R., & Kakar, S. S. (2020). Withaferin A: A potential therapeutic agent against COVID-19 infection. *Journal of Ovarian Research*, 13(1), 79. <https://doi.org/10.1186/s13048-020-00684-x>
- Sundar, D., Yu, Y., Katiyar, S. P., Putri, J. F., Dhanjal, J. K., Wang, J., Sari, A. N., Kolettas, E., Kaul, S. C., & Wadhwa, R. (2019). Wild type p53 function in p53Y220C mutant harboring cells by treatment with Ashwagandha derived anticancer withanolides: Bioinformatics and experimental evidence. *Journal of Experimental & Clinical Cancer Research*, 38(1), 103. <https://doi.org/10.1186/s13046-019-1099-x>
- Tai, W., He, L., Zhang, X., Pu, J., Voronin, D., Jiang, S., Zhou, Y., & Du, L. (2020). Characterization of the receptor-binding domain (RBD) of 2019 novel coronavirus: Implication for development of RBD protein as a viral attachment inhibitor and vaccine. *Cellular & Molecular Immunology*, 17(6), 613–620. <https://doi.org/10.1038/s41423-020-0400-4>
- Tortorici, M. A., & Velesler, D. (2019). Structural insights into coronavirus entry. *Advances in Virus Research*, 105, 93–116. <https://doi.org/10.1016/bs.aivir.2019.08.002>
- Walls, A. C., Park, Y. J., Tortorici, M. A., Wall, A., McGuire, A. T., & Velesler, D. (2020). Structure, function, and antigenicity of the SARS-CoV-2 spike glycoprotein. *Cell*, 181(2), 281–292. <https://doi.org/10.1016/j.cell.2020.02.058>
- Wan, Y., Shang, J., Graham, R., Baric, R. S., & Li, F. (2020). Receptor recognition by the novel coronavirus from Wuhan: An analysis based on decade-long structural studies of SARS Coronavirus. *Journal of Virology*, 94(7). <https://doi.org/10.1128/JVI.00127-20>
- Wang, Q., Zhang, Y., Wu, L., Niu, S., Song, C., Zhang, Z., Lu, G., Qiao, C., Hu, Y., Yuen, K. Y., Wang, Q., Zhou, H., Yan, J., & Qi, J. (2020). Structural and functional basis of SARS-CoV-2 entry by using human ACE2. *Cell*, 181(4), 894–904. <https://doi.org/10.1016/j.cell.2020.03.045>
- WHO. (2020). World Health Organization “Solidarity” clinical trial for COVID-19 treatments. <https://www.who.int/emergencies/diseases/novel-coronavirus-2019/global-research-on-novel-coronavirus-2019-ncov/solidarity-clinical-trial-for-covid-19-treatments>
- Widodo, N., Kaur, K., Shrestha, B. G., Takagi, Y., Ishii, T., Wadhwa, R., & Kaul, S. C. (2007). Selective killing of cancer cells by leaf extract of Ashwagandha: Identification of a tumor-inhibitory factor and the first molecular insights to its effect. *Clinical Cancer Research: An Official Journal of the American Association for Cancer Research*, 13(7), 2298–2306. <https://doi.org/10.1158/1078-0432.CCR-06-0948>
- Widodo, N., Priyandoko, D., Shah, N., Wadhwa, R., & Kaul, S. C. (2010). Selective killing of cancer cells by Ashwagandha leaf extract and its component withanone involves ROS signaling. *PLoS One*, 5(10), e13536. <https://doi.org/10.1371/journal.pone.0013536>
- Wu, K., Peng, G., Wilken, M., Geraghty, R. J., & Li, F. (2012). Mechanisms of host receptor adaptation by severe acute respiratory syndrome coronavirus. *Journal of Biological Chemistry*, 287(12), 8904–8911. <https://doi.org/10.1074/jbc.M111.325803>
- Yu, Y., Katiyar, S. P., Sundar, D., Kaul, Z., Miyako, E., Zhang, Z., Kaul, S. C., Reddel, R. R., & Wadhwa, R. (2017). Withaferin-A kills cancer cells with and without telomerase: Chemical, computational and experimental evidences. *Cell Death & Disease*, 8(4), e2755. <https://doi.org/10.1038/cddis.2017.33>
- Zhang, Q., Chen, C. Z., Swaroop, M., Xu, M., Wang, L., Lee, J., Wang, A. Q., Pradhan, M., Hagen, N., Chen, L., Shen, M., Luo, Z., Xu, X., Xu, Y., Huang, W., Zheng, W., & Ye, Y. (2020). Heparan sulfate assists SARS-CoV-2 in cell entry and can be targeted by approved drugs in vitro. *Cell Discovery*, 6(1), 1–14. <https://doi.org/10.1038/s41421-020-00222-5>
- Zhou, P., Yang, X. L., Wang, X. G., Hu, B., Zhang, L., Zhang, W., Si, H. R., Zhu, Y., Li, B., Huang, C. L., Chen, H. D., Chen, J., Luo, Y., Guo, H., Jiang, R. D., Liu, M. Q., Chen, Y., Shen, X. R., Wang, X., ... Shi, Z. L. (2020). A pneumonia outbreak associated with a new coronavirus of probable bat origin. *Nature*, 579(7798), 270–273. <https://doi.org/10.1038/s41586-020-2012-7>